- 1 Title: Biomimetic sensory feedback through peripheral nerve stimulation improves dexterous use of a
- 2 bionic hand
- 3 Authors: J. A. George^{1*†}, D. T. Kluger^{1†}, T. S. Davis², S. M. Wendelken¹, E. V. Okorokova³, Q. He³, C. C.
- 4 Duncan⁴, D. T. Hutchinson⁵, Z. C. Thumser⁶, D. T. Beckler⁶, P. D. Marasco⁶, S. J. Bensmaia³, G. A. Clark^{1*}
- 5 Affiliations:
- 6 ¹Department of Biomedical Engineering, University of Utah, Salt Lake City, UT, 84112
- 7 Department of Neurosurgery, University of Utah, Salt Lake City, UT, 84112
- 8 ³Department of Organismal Biology and Anatomy, University of Chicago, Chicago, IL, 60637
- 9 ⁴Department of Physical Medicine and Rehabilitation, University of Utah, Salt Lake City, UT, 84112
- ⁵Department of Orthopaedics, University of Utah, Salt Lake City, UT, 84112
- ⁶Department of Biomedical Engineering, Cleveland Clinic, Cleveland, OH, 44195
- 12 *To whom correspondence should be addressed: Jacob.George@utah.edu, Greg.Clark@utah.edu
- 13 †Contributed equally
- 14 **Abstract**: We describe use of a bi-directional neuromyoelectric prosthetic hand that conveys biomimetic
- 15 sensory feedback. Electromyographic recordings from residual arm muscles were decoded to provide
- independent and proportional control of a 6-degree-of-freedom prosthetic hand and wrist the DEKA
- 17 "LUKE" Arm. Activation of contact sensors on the prosthesis resulted in intraneural microstimulation of
- 18 residual sensory nerve fibers through chronically implanted Utah Slanted Electrode Arrays, thereby
- evoking tactile percepts on the phantom hand. With sensory feedback enabled, the participant exhibited
- 20 greater precision in grip force and was better able to handle fragile objects. With active exploration, the
- 21 participant was also able to distinguish between "small" and "large" objects and between "soft" and
- 22 "hard" ones. Importantly, when the sensory feedback was biomimetic designed to mimic natural sensory
- 23 signals the participant was able to identify the objects significantly faster than with use of traditional
- 24 encoding algorithms that depended on only the present stimulus intensity. Thus, artificial touch can be
- 25 sculpted by patterning the sensory feedback, and biologically-inspired patterns elicit more interpretable
- and useful percepts.
- 27 One Sentence Summary: To achieve full dexterity, bionic hands require sensory feedback; artificial
- sensory signals that mimic natural ones are more intuitive and useful.
- 29 MAIN TEXT
- 30 Introduction
- 31 State-of-the-art upper-limb prostheses have become capable of mimicking many of the movements and
- grip patterns of endogenous human hands (1-3). Although these devices have the capabilities to replace
- 33 much of the motor function lost after hand amputation, the methods for controlling and receiving
- 34 feedback from these prosthetic limbs are still primitive (4, 5). The advent of neuromuscular implant
- 35 systems capable of recording efferent motor activity and stimulating afferent sensory nerve fibers
- improves the transfer of sensorimotor information to and from a user's peripheral nervous system, paving
- 37 the way for more dexterous bionic hands (6–9).
- 38 Conveying sensory feedback through an electrical interface with the peripheral nervous system has been
- 39 shown to confer functional benefits (9–16). However, demonstrations of these improvements are limited,
- 40 and the sensory encoding algorithms themselves are often unsophisticated. The human hand is

innervated by several types of tactile nerve fibers that each respond to different aspects of skin deformations. Manual interactions generally activate all of the fiber types, and tactile percepts are shaped by complex spatiotemporal patterns of activation across the different afferent populations (17, 18). One of the striking features of the aggregate afferent activity is the massive phasic bursts during the onset and offset and contact, and the far weaker response during maintained contact (19-22). Strikingly, most extant sensory encoding mechanisms track sensor output (e.g., the absolute pressure, force, or torque from a prosthetic device) by modulating stimulation intensity and thus disregard this important and salient aspect of natural sensory feedback (9, 10, 12, 23-29). To the extent that artificially induced sensory signals mimic natural ones, they are likely to elicit more naturalistic percepts and confer greater dexterity to the user (15, 30).

In the present study, we first demonstrate that closed-loop sensory feedback improves performance on dexterous tasks and enables novel sensory capabilities during active manipulation of objects. We then show that artificial sensory experiences are enriched when the stimulation regimes are designed to mimic the natural patterns of neuronal activation that are evoked during manual interactions with a native hand. These results constitute an important step towards the development of dexterous bionic hands and have broad implications for neural interfaces and prosthetic devices.

Results

We implanted one Utah Slanted Electrode Array (USEA) in the median nerve and another in the ulnar nerve, plus eight electromyographic recording leads (iEMGs) in the forearm muscles of an individual with a transradial amputation halfway between the wrist and elbow. The participant used this neuromyoelectric interface to control and sense through a state-of-the-art dexterous, sensorized prosthetic hand and wrist ("LUKE" Arm, DEKA) (Fig. 1). Control signals were obtained by using the filtered iEMG recordings as input to a modified Kalman filter (29, 31). The participant was able to control all 6 DOFs of the prosthesis independently, proportionally and simultaneously in real-time, achieving comparable performance to clinically-available prosthetics in the "modified Box and Blocks" test (32) (Fig. S1) – a standard test of manual dexterity – and comparable efficiency to that of able-bodied subjects in a novel foraging task (33) (Fig. S2). Recordings of muscle activation remained reliable over the entire duration of the study (14 months). Using muscle recordings rather than neural ones as control signals eliminates the problem of stimulation artifacts and allows for uncompromised sensory feedback.

Electrical stimulation of the residual nerves evokes sensations on the phantom hand

Electrical stimulation of the residual nerves through the chronically implanted USEAs evoked localized sensations that were experienced on the phantom hand. The participant reported up to 119 sensory percepts distributed over the hand and varying in their quality (Fig. 2 and Fig. S3). As might be expected given the known patterns of innervation of the skin, a preponderance of percepts originated in the fingers and particularly the fingertips. The quality of the percepts also varied; some were described as "vibration" (36%), "pressure" (29%), or "tapping" (3%), which likely were associated with activation of cutaneous tactile nerve fibers; others as pain (16%), presumably reflecting activation of nociceptive fibers; and a few as "tightening" (12%) and joint movement (3%), presumably reflecting activation of proprioceptive nerve fibers such as muscle afferents. Activation of contact sensors on the prosthetic hand triggered stimulation of individual USEA electrodes or groups of USEA electrodes with congruent receptive fields. For example, when contact was made with the index fingertip sensor, current was delivered through USEA electrodes with projection fields on the index fingertip of the phantom; that way, when the prosthetic index fingertip made contact with an object, the participant experienced a sensation on the index fingertip.

Sensory feedback improves grasping performance

85 The grip force required to grasp an object depends on its mass and on the coefficient of friction between 86 skin and object: Heavy and slippery objects are gripped with more force than are light, high-friction ones 87 (34). With our native hands, we are exquisitely proficient at exerting just enough pressure on an object to 88 grasp it, an ability for which we rely on the sense of touch (34).

Some tests of manual dexterity do not benefit from tactile feedback. For example, performance on the "modified Box and Blocks" test is only slightly improved with touch because visual feedback is available and no penalty is incurred for exerting too much force on an object. Other tests of manual dexterity are highly dependent on tactile feedback, however. In one such test, a participant moves an object from one location to another, as in the "modified Box and Blocks" test (Fig. S1). However, the object is "fragile" and "breaks" if squeezed too hard (Fig. S4)(35, 36). The participant moved the object without breaking it significantly more often with sensory feedback than without (32/40 times vs 22/40 times; Pearson's chisquare test; p = 0.017; Fig 3) and did so more rapidly $(9.13 \pm 0.44 \text{ s vs } 11.14 \pm 0.49 \text{ seconds per trial; t-test,}$ *p* < 0.001; Fig. 3).

98 Performance of activities of daily living (ADLs) often involves dividing attention between multiple 99 simultaneous subtasks - e.g., holding a jar while twisting off its lid - so sensory feedback that is 100 attentionally demanding is inappropriate (37). To test whether the sensory feedback conveyed through nerve stimulation was resistant to divided attention, we had subjects perform the fragile-object test while 102 counting backwards. We found that the feedback-induced boost in performance was maintained with 103 divided attention, but only the effect on duration remained statistically significant in this condition (5.91 104 \pm 0.20 s vs 7.68 \pm 0.42 s; t-test, p < 0.001; Fig. 3).

Another way to assess the impact of sensory feedback on object interactions is to characterize the degree to which we exert a consistent amount of force on an object upon repeated grasping (38). To test this capability, we had the participant repeatedly grasp a load cell with the prosthetic hand. Sensory feedback was provided on some experimental blocks but not others. The participant's grip performance was more precise with sensory feedback than without, as evidenced by less variable grip force on 6 of 8 objects (Fig. 4). Furthermore, sensory feedback significantly reduced the coefficient of variation (ratio of grip precision to grip force) across all objects (Fig. 4; Fig. S5 shows the standardized Grasping Relative Index of Performance, GRIP, for this test) (38).

113 Sensory feedback enables haptic perception

89

90

91

92

93

94 95

96

97

101

105

106

107

108

109

110

111

112

114

115

116

117

118

119

120

121

122

123

124

125

When we manipulate objects, we acquire information about their shape, size, and texture through sensory signals from our hands (39, 40). Haptic perception relies on an interplay between exploratory movements and the sensory consequences of those movements (41). To assess the degree to which the prosthesis could convey object information, we developed a closed-loop sensorimotor task in which the participant actively manipulated one of two objects with the prosthetic index finger (Fig. S6). Stimulation was at a fixed frequency and amplitude, and was delivered as long as contact with the object was maintained. On each trial, one of two objects was presented – a golf ball or a (larger) lacrosse ball – and the participant's task was to report the size of the object (small vs. large). Alternative sensory cues were reduced or eliminated by having the arm mounted externally on a table (rather than being worn by the subject) and by having the subject wear an eye mask and headphones. The participant was able to perform this task almost perfectly with the sensory feedback, correctly reporting the size on 31 out of 32 object presentations (binomial test; p < 0.0001).

126 To further assess haptic perception, we developed a closed-loop sensorimotor task in which the 127 participant actively manipulated one of two objects - a soft foam block or a hard plastic block - and 128 discriminated the compliance (soft vs. hard) (Fig. S7). In this experiment, the amplitude of electrical 129 stimulation increased linearly with the output of the sensor. The participant was able to distinguish

- 130 between the two objects significantly better than chance (60/80 trials; binomial test; p < 0.0001) and did
- 131 so after squeezing the object several times (Fig. 5), highlighting the interplay between motor behavior and
- 132 sensory feedback.
- 133 Biomimetic peripheral nerve stimulation improves object discrimination
- 134 In the studies described above, sensory feedback provided either a contact signal or a signal proportional
- 135 to the contact force. Although both regimes of stimulation led to significant improvements in closed loop
- 136 sensorimotor tasks, neither regime is liable to produce naturalistic patterns of activation in the nerve.
- 137 Indeed, interactions with objects are characterized by a strong burst of activation at the onset and offset
- 138 of contact and much weaker activation during maintained contact (42). This initial onset conveys
- 139 important information about the shape of the object (40). The aggregate response of tactile nerve fibers
- 140 is determined not only by the degree to which the skin is indented, but also the rate at which the skin is
- 141 indented, and the latter component dwarfs the former one.
- 142 We therefore sought to implement a sensory feedback algorithm that incorporates this temporal property
- 143 of natural tactile signals. As a first-order approximation, we developed a sensory feedback algorithm in
- 144 which the intensity of stimulation was proportional not just to the contact force but also to its rate of
- 145 change. This first-order biomimetic algorithm leads to stronger stimulation at the contact onset, when the
- 146 rate of change is highest, to mimic the phasic bursts observed in natural nerve activation during contact
- 147 transients. To test this simple biomimetic algorithm, we had the participant discriminate the size and
- 148 compliance of objects, and we compared his performance with that using the standard sensory encoding
- 149 algorithms (contact tracking, force tracking). We found that the participant was able to perform these
- 150 tasks significantly faster with the biomimetic feedback than with its non-biomimetic counterparts.
- 151 Biomimetic sensory feedback improved response time by 24% for size discrimination (11.78 ± 0.75 s vs
- 152 8.94 \pm 0.79 s; t-test; p < 0.05; Fig. 5) and by 44% for compliance discrimination (14.16 \pm 1.05 s vs 7.91 \pm
- 153 0.81 s; t-test; p < 0.005; Fig. S7).
- 154 In the above implementation of biomimetic feedback, the peak intensity of stimulation was higher than
- 155 with non-biomimetic feedback because the overall charge was approximately matched. One possibility,
- 156 then, was that the improvement in performance with biomimetic feedback was a consequence of the
- 157 higher peak stimulation intensity. Although a higher peak firing rate might itself be more biomimetic,
- 158 improved discrimination would not necessarily depend on differences in temporal firing patterns between
- 159 the biomimetic and non-biomimetic encoding schemes. To distinguish between these possibilities, we
- 160 implemented a version of the biomimetic algorithm such that the peak stimulation intensity (pulse
- 161 amplitude and frequency) was matched to that of the non-biomimetic algorithms. Even with matched
- 162 peak intensity, the biomimetic feedback led to a 46% improvement in performance (7.56 ± 1.08 s vs 4.64
- 163 \pm 0.77 s; t-test; p < 0.005; Fig. 5). Another potential confound is that biomimetic algorithm might peak
- faster than the non-biomimetic ones, leading to faster performance. However, the improvement in 164
- 165 response time was on a longer time scale than the shift in peak stimulation, so this effect was not a trivial
- consequence of the timing of stimulation. Rather, it reflects an improvement in the intuitiveness and 166
- informativeness of the artificial sensory signals, which capture some of the essential temporal 167
- 168 characteristics of natural tactile signals.
- 169 The above results suggest that dynamics of the response evoked through electrical stimulation – if it
- 170 mimics a natural response – can lead to more interpretable and useful sensory feedback. However, the 171
- above biomimetic algorithm captured some aspects of the natural tactile feedback namely the increase
- 172 in sensitivity to contact transients - but not others, borne out of the idiosyncratic properties of the
- 173 different classes of tactile nerve fibers and their respective innervation densities. In light of this, we tested 174 another sensory encoding algorithm that sought to more faithfully mimic natural nerve activations. In
- 175 brief, this algorithm is designed to reflect the measured sensitivity of populations of nerve fibers to skin

- indentation and its two derivatives (rate and acceleration) (19). With this second-order biomimetic
- feedback, the participant identified object compliance 56% faster than with the traditional linear feedback
- 178 (6.71 \pm 1.47 s vs 2.93 \pm 1.37 s; t-test; p < 0.05; Fig. 5). These results further demonstrate that biomimicry
- improves the intuitiveness of the artificial sensory feedback.
- 180 Participant successfully performed a variety of activities of daily living
- An important concern in laboratory demonstrations of neuroprosthetic control is whether tasks that are
- used to assess the performance of the prosthesis are ecologically valid. With regards to the present study,
- will improvements in performance with sensory feedback on laboratory tasks translate to improved
- performance on ADLs? We evaluated this by having the participant complete several ADLs over three days
- of testing. With just the prosthesis alone or in conjunction with his intact hand, he performed basic ADLs
- (feeding and dressing) (43), instrumental ADLs (housework, meal preparation, and technology use) (44),
- and ADLs that he had found challenging without the prosthesis (loading a pillow into a pillowcase,
- hammering, donning and doffing a ring) (Fig. 6). Improvements are difficult to quantify with ADLs, but the
- participant noted sensory feedback was particularly useful when manipulating fragile objects (e.g., eggs,
- grapes) and spontaneously reported that he enjoyed the sensation of "feeling" objects in his hand.
 - Discussion

- In the present study, we demonstrate that artificial sensory feedback improves fine motor control and
- confers to the user the ability to sense object properties though a bionic hand. Furthermore, these
- artificial sensory experiences are enriched when the sensory feedback is designed to mimic the nervous
- system's natural language. By capturing some of the essential characteristics of natural tactile signals,
- 196 biomimetic stimulation improves the intuitiveness and informativeness of the sensory feedback, as
- 197 evidenced by swifter object discrimination capabilities.
- 198 The present results build on previous work showing that sensory feedback leads to improved grip and
- handling of fragile objects (10). We extend these previous findings by showing that grasp force is achieved
- faster and more accurately, and that fragile objects are transferred faster with than without sensory
- 201 feedback. Importantly, these improvements are augmented when the sensory feedback is biomimetic.
- 202 Although previous studies had demonstrated that object properties can be sensed through a prosthetic
- 203 hand (12), we extend these previous findings to a different sensorimotor task compliance discrimination
- 204 and directly demonstrate the improvement of biomimetic feedback relative to its non-biomimetic
- 205 counterpart. In this respect, our work is consistent with a recent study showing that biomimetic
- stimulation leads to more naturalistic percepts, leads to greater embodiment, and improves performance
- 207 on object manipulation tasks (15, 30). In the present study, we extend these previous findings to a new
- technology and a new task, an important replication of the benefits of sensory feedback and biomimicry,
- given that the relevant studies thus far have involved a single participant (13, 30, 45, 46).
- Amputees have expressed a desire for sensory feedback to reduce their dependence on visual feedback
- 211 (37). The ability to feel grip force while grasping and holding objects is the most important aspect of
- sensory feedback for amputees (47). The sensory feedback provided here allows the participant to
- 213 perform object discrimination tasks without visual or auditory feedback and enables the participant to
- 214 exert grip forces more precisely.
- 215 In the limit, ideal sensory peripheral nerve interfaces and encoding algorithms would activate each
- afferent nerve fiber selectively and independently, so as to replicate the spatiotemporal pattern of neural
- discharges that would be transmitted from an intact hand. The ability of different USEA electrodes to
- activate a large number of different percepts (Fig. 2) increases the ability to provide more biomimetic
- sensory input. The present experiments utilized relatively simple receptive fields and sensorimotor tasks
- in order to study the importance of temporal aspects of sensory encoding at a population level in isolation

- of additional factors, and hence did not fully explore these capabilities. However, such capabilities may
- 222 prove increasingly useful with richer sensorimotor tasks and with the advent of prosthetic hands with
- 223 greater numbers and varieties of sensors.
- 224 In addition to sensorimotor functional improvements, closed-loop sensorized prostheses often bring
- psychological benefits (9, 10, 29, 48–50). The same participant in this study reported decreased phantom
- pain and increased embodiment of the prosthesis as a result of the sensory feedback (29). After the study,
- the participant highlighted the emotional impact of artificial touch when he used the bionic hand to shake
- 228 hands with his wife and felt her touch through it for the first time. The functional and emotional benefits
- of dexterous motor control and biomimetic sensory feedback are likely to be further enhanced with long-
- term use, and efforts are underway to develop a portable take-home system (51).

Materials and Methods

232 Study design

- 233 We considered the participant for this chronic implant study due to the transradial level of his amputation,
- 234 his willingness to volunteer, and overall good health. Termination of the study and explantation of the
- electrodes were voluntary, or would occur if the implants were causing a health risk as indicated by a
- 236 qualified physician, or at 14 months after the implant date. Previous studies from this group (6, 52, 53)
- were limited in duration (less than 5 weeks) for safety considerations; because no health risks emerged
- from these previous studies, the University of Utah Institutional Review Board and the participant agreed
- to a 14-month duration for this study.
- 240 The experiments performed in this study were completed in 2–3-hour sessions, 1–3 times a week, across
- the 14-month duration of the study. The number of replicates per experiment was matched to that of
- 242 previous studies involving fragile-object manipulation (10), object discrimination (45), and the Grasping
- 243 Relative Index of Precision (38). Data were considered outliers if they fell outside three standard
- 244 deviations from the mean (38).
- 245 Human subject and implanted devices
- A male left transradial amputee, whose amputation occurred 13 years prior to the onset of the study,
- 247 underwent surgeries and performed experiments with informed consent and under protocols approved
- 248 by the University of Utah Institutional Review Board and the Department of Navy Human Resources
- 249 Protection Program. Under general anesthesia, two 100-electrode Utah Slanted Electrode Arrays (USEAs)
- were implanted in the median and ulnar nerves of the residual limb, proximal to the elbow, and eight
- electromyographic recording leads (iEMGs), with four electrical contacts each, were implanted in the
- upper forearm with attempted targeting of each lead to different lower-arm extensor or flexor muscles.
- 253 Additional information and figures regarding the devices and implantation procedure can be found in the
- supplemental materials and (29), which reports on the same participant in this study.
- 255 Decoding motor intent
- 256 Motor intent was decoded from residual forearm muscles recorded at 1 kHz while the participant actively
- 257 mimicked prosthetic hand movements, as previously reported in (6, 29, 31). Every 33 ms, the mean
- absolute value (MAV) over a 300-ms window was calculated for the 32 iEMG electrodes as well as the 496
- possible differential pairs. A total of 528 features were generated (MAV for 32 single-ended + 496
- differential pairs). In order to save computational time and reduce potential overfitting, the 528 features
- were then down-selected to the best 48 features using a Gram-Schmidt channel-section algorithm (54).
- 262 These 48 features served as an input to a modified Kalman-filter-based (MKF) decode which utilizes
- customizable, non-unity thresholds and gains (29, 55). The output of the MKF was used to directly control
- the position or velocity of the 6 DOFs of the prosthesis. The ability to proportionally control position or

- 265 velocity was toggled on a DOF-by-DOF basis. More information regarding the prosthetic control algorithm
- can be found in (55) and the supplemental material.
- 267 Mapping of USEA-evoked percepts
- 268 Electrical stimulation was delivered via USEAs using the Ripple, LLC Grapevine System with Micro2+Stim
- front ends. All stimulation was delivered as biphasic, cathodic-first pulses, with 200–320-µs phase
- durations, and a 100-us interphase duration. The stimulation frequency varied between 10–500 Hz, and
- stimulation amplitudes were in the range of 1–100 μ A.
- 272 USEA stimulation threshold maps were collected roughly every 4–8 weeks, during which each electrode
- of the USEAs was stimulated in isolation at increasing amplitudes. Electrodes that evoked a sensory
- percept at less than 100 μA were noted, and the location, quality, and intensity of each percept was
- documented as well as the threshold amplitude at which the percept was evoked. For these mappings,
- stimulation was delivered in a pulsed fashion, with a 500-ms train of 100-Hz stimulation being delivered
- every second. Additional descriptions for electrode mapping (6) and the stimulation parameters we
- used (29) exist elsewhere. Sensory percepts were stable over the course of these experiments and
- persisted 14 months after the implant (Fig. S8). More information regarding the stability of the USEA-
- evoked percepts is available in the supplemental material.
- 281 Encoding sensory feedback
- 282 Stimulation through a single USEA electrode typically evoked a single percept with a distinct receptive
- field (e.g., sensations were isolated to just the index finger, or just the middle finger, but not both fingers).
- 284 Occasionally stimulation of a single USEA electrode would evoke multiple percepts in distinct receptive
- fields (e.g., stimulation of a single USEA electrode evoked sensations on both the index and middle
- 286 fingers); these electrodes with multiple distinct percepts were not used for real-time sensory feedback.
- 287 The distinctly evoked percepts were then assigned to a single contact (cutaneous) or motor
- 288 (proprioceptive) sensor on the prosthesis with a corresponding receptive field. For example, if stimulation
- 289 through USEA electrode X evoked a pressure-like percept on the middle finger, and if separately
- 290 stimulating through USEA electrode Y also evoked a percept on the middle finger, then both electrodes X
- and Y would be assigned to the middle finger contact sensor on the prosthesis. We stimulated between 1
- and 12 USEA electrodes that had overlapping receptive fields with a given sensor on the prosthesis (Table
- 293 1). Due to the time-intensive nature of assigning all electrodes, a subset of sensors on the prosthesis were
- used for each task; the specific sensors used for a particular task are detailed in the corresponding section
- for that task in the methods. Activation of sensors resulted in biphasic, charge-balanced stimulation (200-
- 296 μs or 320-μs phase durations, cathodic-first, with a 100-μs interphase duration). We encoded percept
- intensity by modulating the frequency or current amplitude of stimulation with either linear or biomimetic
- 298 encoding algorithms (see section below). For all encoding algorithms, the intensity of the sensation
- increased with increasing stimulation amplitude and frequency, but there were no reported changes in
- 300 perceptive field location or sensory modality.
- 301 Stimulation parameters were adjusted at the start of each experimental session in order to maximize the
- 302 naturalism and perceived intensity range of the stimulation. To the extent possible, the participant's
- sensory experience (e.g., perceived intensity range, perceptive field, etc.) was kept consistent across days.
- 304 Stimulation typically produced natural-feeling pressure sensations on the palmar aspects of the hand. The
- 305 exact parameters (electrodes, encoding algorithm, amplitude, frequency, pulse duration) used for each
- task are summarized in Table 1.
- 307 Sensory encoding algorithms

For binary sensory encoding, the stimulation was fixed at the specified amplitude (100 μA, 320 μS) and frequency (100 Hz) as long as any contact was made. For traditional, linear sensory encoding, the stimulation frequency and amplitude increased based solely on the absolute sensor value. For biomimetic 1 sensory encoding, the stimulation frequency and amplitude increased based on the absolute sensor value and on positive rate of change of the sensor; stimulation tracked the current sensor value plus 10 times any positive finite difference between the current and previous sensor value. For scaled, traditional, linear sensory feedback, the stimulation frequency and amplitude were multiplied by a constant factor (=2) such that the range was comparable to that of the biomimetic stimulation (Fig. 5). Stimulation amplitude and frequency increased together over their respective ranges (see Table 1 and Table 2).

The biomimetic 2 sensory encoding algorithm was developed from recordings of non-human primate cutaneous afferents in response to physical contact with the fingertip (19). This computationallyinexpensive model describes the instantaneous firing rate (i.e., stimulation frequency) of the afferent population using the contact stimulus position, velocity and acceleration. Similar to other biomimetic algorithms (30), the biomimetic 2 sensory encoding algorithm leverages TouchSim (56) to simulate the responses of all tactile fibers to any spatiotemporal deformation of the skin of the hand. This model – dubbed TouchMime - provides a more computationally-efficient approach to the aggregate response of the nerve to time-varying pressure applied to the fingertip, allowing for high-accuracy biomimetic sensory encoding in real-time. In addition, the parameters of the model were tuned for the sampling rate of the DEKA "LUKE" Arm sensors (30 Hz) and for USEA stimulation (i.e., intrafascicular stimulation at 30 Hz) at a fixed, suprathreshold stimulation amplitude, further improving the accuracy of the biomimetic encoding (19). Additional details regarding the model development and validation can be found in (19).

329 Both models presented here are distinct from those used in (30). The biomimetic 1 algorithm concurrently 330 modulates frequency and amplitude most closely replicating the responses of populations of slowly 331 adapting type 1 (SA1) and rapidly adapting (RA) fibers. The biomimetic 2 algorithm provides a more 332 faithful replication of a complete aggregate nerve response, keeping the population size constant (fixed 333 stimulation amplitude) and mimicking the aggregate firing rate of SA1, RA, and Pacinian fibers within that 334 population of the nerve. Both models are computationally efficient, allowing for real-time biomimetic 335 sensory encoding. Analytic formulations for each encoding algorithm are provided in Table 2.

336 We did not attempt to measure the intuitiveness or naturalism of the sensory encoding algorithms, nor 337 did we track the subject's ability to interpret this feedback. Experimental sessions were kept under two 338 hours and no learning effects were observed in this time frame.

339 Fragile-object test

308

309

310 311

312

313

314

315

316

317

318

319

320

321

322

323

324

325

326

327

328

341

347

348

349

350

351

352

340 The fragile-object test (originally introduced in ref. (35)), has been used as a variant of the "modified Box and Blocks" test (36) to show the benefits of sensory feedback (14, 30, 36). Our implementation of this 342 test differs from its predecessors in that the object is much heavier and the ratio between the weight and 343 breaking force is much smaller, rendering the overall task more difficult. Indeed, in ref. (36), the fragile 344 object weighed 8 g and broke if a force of 10.7 ± 1 N was applied to it (ratio of 1.34 N/g), and in refs. (14, 345 30), the object weighed $^{\sim}80$ g broke with a force of 1.23 ± 0.02 N (ratio of 0.15 N/g). In contrast, the object 346 used in this study weighs 630.57 g and breaks at 14.79 ± 0.34 N (ratio of 0.02 N/g).

The participant used only thumb abduction/adduction, and artificial sensory feedback was provided based on the thumb contact sensor. Trial failure was defined as "breaking" the object, which occurred when the compression force exceeded 14.79 ± 0.34 N, or an inability to move the object in 30 s. Trial success was defined as a trial in which the participant lifted and placed the unbroken object within an adjacent circle on the table (~10 cm away) within 30 s. In half of the sets, the participant was intentionally distracted by having to count backwards by twos from a random even number between 50 and 100.

- 353 A single trial was performed once every minute. A single experimental block consisted of 8 trials with or
- without artificial sensory feedback. The participant completed five experimental blocks with and without
- sensory feedback, for both the basic and distracted conditions. The experimental blocks were
- 356 counterbalanced in order to reduce order effects. Under all conditions, the participant was able to use
- audiovisual feedback to help locate and grasp the object, as well as to identify when the object broke.
- 358 Statistical analyses were run separately for the basic and distracted conditions. A 50% binomial test was
- used to determine if performance was significantly greater than chance alone. For comparison of
- 360 completion time for the successful trials, response times showed no deviations from normality (Anderson-
- 361 Darling, Jarque-Bera and Lilliefors tests). Unpaired t-tests (unequal sample size due to different success
- rates) were then used to compare completion times.
- 363 Object-discrimination tasks
- For size discrimination, the participant had to distinguish between a "large" lacrosse ball and a "small"
- golf ball (Fig. S6). The two objects were chosen so that they represented real-world interactions,
- minimized differences in compliance, and maximized differences in size while still requiring some degree
- of active flexion to make contact. Relative to the index finger's full range of motion, the large object
- required a 19% decrease in joint angle to make contact, and the small object required a 49% decrease.
- Response time was measured from the start of the trial to when the participant verbally reported the
- object's size.
- For compliance discrimination, the participant had to distinguish between a "soft" foam block and a
- "hard" plastic block (Fig. S7). The soft block was cut to match the size of the hard block so that stimulation
- due to initial contact occurred at the same degree of index flexion. Response time was measured from
- the start of stimulation (i.e., measurable contact was made with the object and the participant felt the
- object) to the time when the participant verbally reported the object's compliance.
- 376 We did not attempt to quantify how many levels of size and compliance the subject was able to
- discriminate. With traditional linear feedback, the just-noticeable difference of the neural stimulation
- would bound the discrimination capabilities. Instead, we focused on quantifying improvements in the
- intuitiveness of the sensory feedback (measured by response time) when biomimetic stimulation regimes
- are employed.
- For both, the output of the modified Kalman filter was used to directly control the position of the index
- finger. Position control (i.e., postural control) provided improved performance relative to velocity control
- (Fig. S6), which is consistent with the natural encoding schemes of the hand (57). The participant received
- 384 cutaneous sensory feedback from the index contact sensor; proprioceptive sensory feedback was not
- provided, although endogenous proprioception of residual forearm muscles and efference copy may have
- been present. The participant was blindfolded, wearing headphones, and the physical prosthesis was
- detached from his residual limb so that external cues about the object were eliminated.
- A single trial was performed once every minute. For each trial, the participant was given 30 s to complete
- the task. A single experimental block consisted of 8 trials using a single algorithm. The participant
- 390 completed two experimental blocks for each size discrimination algorithm and two to six experimental
- blocks for each compliance discrimination algorithm. The order of the objects was pseudorandomized
- 392 such that equal numbers of both appeared in the experimental block. The experimental blocks were
- 393 counterbalanced in order to reduce order effects.
- 394 Statistical analyses were run separately for each algorithm comparison. Due to limited time with the
- participant, direct comparisons were limited to biomimetic 1 vs traditional linear, biomimetic 1 vs scaled
- traditional linear, and biomimetic 2 vs scaled traditional linear. A 50% binomial test was used to determine
- 397 if performance was significantly greater than chance alone. For algorithm comparisons, response times

- showed no deviations from normality (Anderson-Darling, Jarque-Bera and Lilliefors tests). Paired t-tests
- were then used for these comparisons on a trial-by-trial basis in order to control for order effects and
- sensory adaptation (58). Statistical analysis of response times with biomimetic and non-biomimetic
- 401 encoding algorithms was confined to algorithms utilizing the same stimulation parameters on the same
- day in order to avoid any variations in evoked sensations that may have occurred across days.
- 403 Grasping Relative Index of Precision test
- A detailed description of the GRIP Test is reported elsewhere (38). In short, a screen was placed between
- 405 the participant's line of sight to the prosthesis and the load cell to eliminate audiovisual cues from the
- 406 prosthetic hand. In contrast to the fragile-object test, the GRIP Test measures the ability to modulate grip
- force without audiovisual feedback. The participant was presented with pictures of one of eight objects
- 408 (Fig. 4) and instructed to grab the load cell with a force appropriate for gripping the object shown in the
- 409 picture. The participant grabbed each of the eight objects 20 times without sensory feedback and 20 times
- with sensory feedback. Outliers and trials with preemptive grasps were not included in the analysis (38).
- 411 Peak grasping forces showed no deviations from normality (Anderson-Darling, Jarque-Bera and Lilliefors
- 412 tests). Unpaired t-tests were used to compare means and Levene's test was used to compare standard
- 413 deviations.
- 414 DEKA "LUKE" Arm & activities of daily living
- 415 The DEKA "LUKE" Arm, as used in this study, has 6 moveable degrees of freedom (Table 3), 6 position
- sensors, and 13 contact sensors (Table 4). The prosthetic is interfaced via a Controller Area Network (CAN)
- 417 communication protocol with 100-Hz update cycles. The accuracy of the movements is dictated by the
- precision of the motor commands (Table 3). For more information regarding the accuracy of the control
- algorithm, see the supplemental material and (55).
- 420 The DEKA "LUKE" Arm, in its transradial configuration, weighs approximately 1.27 kg (59), slightly more
- 421 than that of an intact human hand. There are no temperature or pain sensors on the DEKA "LUKE" Arm.
- 422 Furthermore, electrical stimulation of sensory afferents preferentially activates larger diameter fibers first
- 423 (60), making USEA-evoked pain or temperature percepts uncommon.
- 424 The 6 position sensors correspond to the 6 moveable degrees of freedom. The 13 contact sensors are
- made of 9 torque sensors for contact applied to the fingers and 4 force sensors for contact applied to the
- hand. There is a torque sensor for each digit D2-D5 that detects torque applied to the finger opposing
- flexion (e.g., during grasping of an object) as well as a torque sensor for the lateral portion of D2 (e.g.,
- during a key grip). D1 also has 4 additional torque sensors to detect contact due to adduction, abduction,
- 429 reposition or opposition.
- Activities of daily living were performed with the DEKA "LUKE" Arm mounted to a custom socket fit to the
- residual limb of participant. With just the prosthesis or with in conjunction with his intact hand, the
- 432 participant performed basic ADLs (feeding and dressing) (43), instrumental ADLs (housework, meal
- 433 preparation, and technology use) (44), and ADLs that he had found challenging without the prosthesis
- 434 (loading a pillow into a pillowcase, hammering, donning and doffing a ring) (Fig. 6). All activities of daily
- living were performed with audiovisual feedback to best approximate real-world use. Traditional linear
- sensory feedback was provided because activities of daily living were performed prior to implementing
- 437 the biomimetic encoding algorithms. Due to limited patient time and an inability to precisely quantify
- 438 performance, activities of daily living were not repeated with biomimetic sensory feedback.
- 439 Statistical analyses
- All statistical analyses were run with significance as $\alpha = 0.05$. Data were check for normality to ensure the
- 441 appropriate parametric analysis or non-parametric equivalent was used. Subsequent pairwise analyses

- 442 were corrected for multiple comparisons using the Dunn-Sidák approach. All data are shown as mean ±
- 443 S.E.M. unless otherwise stated.
- 444 Supplemental Materials
- 445 Stability of the Utah Slanted Electrode Array
- 446 Fig. S1. "Modified Box and Blocks" test
- 447 Fig. S2. Prosthesis Efficiency and Profitability task
- 448 Fig. S3. Projected fields of electrically-evoked sensations
- 449 Fig. S4. Fragile-object test
- 450 Fig. S5. Grasping Relative Index of Precision task
- 451 Fig. S6. Size-discrimination task
- 452 Fig. S7. Compliance-discrimination task
- 453 Fig. S8. Stability of USEA-evoked sensations
- 454 References and Notes:
- 455 1. Mobius Bionics, LUKE Arm Detail Page Mobius Bionics (available at http://www.mobiusbionics.com/luke-
- 456 arm/).
- 457 2. Ottobock, bebionic Technical Manual (available at
- 458 http://bebionic.com/distributor/documents/Tech Manual Medium Large Hand1.pdf).
- 459 3. Touch Bionics, User Brochure: i-limb quantum (available at
- 460 http://www.touchbionics.com/sites/default/files/files/MA01374US%20rev.%202%2C%20January%202017%20Use
- r%20Brochure i-limb%20quantum.pdf).
- 462 4. E. Biddiss, T. Chau, Upper-limb prosthetics: critical factors in device abandonment, *Am. J. Phys. Med. Rehabil.*
- **86**, 977–987 (2007).
- 464 5. F. Cordella, A. L. Ciancio, R. Sacchetti, A. Davalli, A. G. Cutti, E. Guglielmelli, L. Zollo, Literature Review on
- Needs of Upper Limb Prosthesis Users, Front. Neurosci. 10 (2016), doi:10.3389/fnins.2016.00209.
- 466 6. S. Wendelken, D. M. Page, T. Davis, H. A. C. Wark, D. T. Kluger, C. Duncan, D. J. Warren, D. T. Hutchinson,
- 467 G. A. Clark, Restoration of motor control and proprioceptive and cutaneous sensation in humans with prior upper-
- limb amputation via multiple Utah Slanted Electrode Arrays (USEAs) implanted in residual peripheral arm nerves,
- 469 *J. NeuroEngineering Rehabil.* **14** (2017), doi:10.1186/s12984-017-0320-4.
- 470 7. T. A. Kuiken, G. Li, B. A. Lock, R. D. Lipschutz, L. A. Miller, K. A. Stubblefield, K. Englehart, Targeted Muscle
- 471 Reinnervation for Real-Time Myoelectric Control of Multifunction Artificial Arms, JAMA J. Am. Med. Assoc. 301,
- 472 619–628 (2009).
- 8. T. A. Kung, R. A. Bueno, G. K. Alkhalefah, N. B. Langhals, M. G. Urbanchek, P. S. Cederna, Innovations in
- 474 Prosthetic Interfaces for the Upper Extremity:, *Plast. Reconstr. Surg.* **132**, 1515–1523 (2013).
- 475 9. M. Schiefer, D. Tan, S. M. Sidek, D. J. Tyler, Sensory feedback by peripheral nerve stimulation improves task
- performance in individuals with upper limb loss using a myoelectric prosthesis, *J. Neural Eng.* **13**, 016001 (2016).
- 10. D. W. Tan, M. A. Schiefer, M. W. Keith, J. R. Anderson, J. Tyler, D. J. Tyler, A neural interface provides long-
- term stable natural touch perception, *Sci. Transl. Med.* **6**, 257ra138 (2014).

- 479 11. G. S. Dhillon, K. W. Horch, Direct neural sensory feedback and control of a prosthetic arm, *IEEE Trans. Neural*
- 480 Syst. Rehabil. Eng. Publ. IEEE Eng. Med. Biol. Soc. 13, 468–472 (2005).
- 481 12. S. Raspopovic, M. Capogrosso, F. M. Petrini, M. Bonizzato, J. Rigosa, G. D. Pino, J. Carpaneto, M. Controzzi,
- 482 T. Boretius, E. Fernandez, G. Granata, C. M. Oddo, L. Citi, A. L. Ciancio, C. Cipriani, M. C. Carrozza, W. Jensen,
- 483 E. Guglielmelli, T. Stieglitz, P. M. Rossini, S. Micera, Restoring natural sensory feedback in real-time bidirectional
- 484 hand prostheses, *Sci. Transl. Med.* **6**, 222ra19-222ra19 (2014).
- 485 13. C. M. Oddo, S. Raspopovic, F. Artoni, A. Mazzoni, G. Spigler, F. Petrini, F. Giambattistelli, F. Vecchio, F.
- 486 Miraglia, L. Zollo, G. Di Pino, D. Camboni, M. C. Carrozza, E. Guglielmelli, P. M. Rossini, U. Faraguna, S. Micera,
- 487 Intraneural stimulation elicits discrimination of textural features by artificial fingertip in intact and amputee humans,
- 488 *eLife* **5** (2016), doi:10.7554/eLife.09148.
- 489 14. F. M. Petrini, G. Valle, I. Strauss, G. Granata, R. Di Iorio, E. D'Anna, P. Čvančara, M. Mueller, J. Carpaneto, F.
- 490 Clemente, M. Controzzi, L. Bisoni, C. Carboni, M. Barbaro, F. Iodice, D. Andreu, A. Hiairrassary, J.-L. Divoux, C.
- Cipriani, D. Guiraud, L. Raffo, E. Fernandez, T. Stieglitz, S. Raspopovic, P. M. Rossini, S. Micera, Six-Month
- 492 Assessment of a Hand Prosthesis with Intraneural Tactile Feedback: Hand Prosthesis, Ann. Neurol. 85, 137–154
- 493 (2019).
- 494 15. L. Zollo, G. D. Pino, A. L. Ciancio, F. Ranieri, F. Cordella, C. Gentile, E. Noce, R. A. Romeo, A. D.
- Bellingegni, G. Vadalà, S. Miccinilli, A. Mioli, L. Diaz-Balzani, M. Bravi, K.-P. Hoffmann, A. Schneider, L.
- Denaro, A. Davalli, E. Gruppioni, R. Sacchetti, S. Castellano, V. D. Lazzaro, S. Sterzi, V. Denaro, E. Guglielmelli,
- 497 Restoring tactile sensations via neural interfaces for real-time force-and-slippage closed-loop control of bionic
- 498 hands, Sci. Robot. 4, eaau9924 (2019).
- 499 16. E. D'Anna, G. Valle, A. Mazzoni, I. Strauss, F. Iberite, J. Patton, F. M. Petrini, S. Raspopovic, G. Granata, R. D.
- 500 Iorio, M. Controzzi, C. Cipriani, T. Stieglitz, P. M. Rossini, S. Micera, A closed-loop hand prosthesis with
- simultaneous intraneural tactile and position feedback, Sci. Robot. 4, eaau8892 (2019).
- 502 17. H. P. Saal, S. J. Bensmaia, Touch is a team effort: interplay of submodalities in cutaneous sensibility, *Trends*
- 503 Neurosci. 37, 689–697 (2014).
- 18. S. Hsiao, Central mechanisms of tactile shape perception, *Curr. Opin. Neurobiol.* **18**, 418–424 (2008).
- 505 19. E. V. Okorokova, Q. He, S. J. Bensmaia, Biomimetic encoding model for restoring touch in bionic hands
- through a nerve interface, *J. Neural Eng.* **15**, 066033 (2018).
- 507 20. G. Westling, R. S. Johansson, Responses in glabrous skin mechanoreceptors during precision grip in humans,
- 508 Exp. Brain Res. **66**, 128–140 (1987).
- 509 21. R. S. Johansson, G. Westling, Programmed and triggered actions to rapid load changes during precision grip,
- 510 Exp. Brain Res. 71, 72–86 (1988).
- 511 22. G. Westling, R. S. Johansson, Factors influencing the force control during precision grip, Exp. Brain Res. 53,
- 512 277–284 (1984).
- 513 23. E. D'Anna, F. M. Petrini, F. Artoni, I. Popovic, I. Simanić, S. Raspopovic, S. Micera, A somatotopic
- 514 bidirectional hand prosthesis with transcutaneous electrical nerve stimulation based sensory feedback, Sci. Rep. 7
- 515 (2017), doi:10.1038/s41598-017-11306-w.
- 516 24. C. Pylatiuk, A. Kargov, S. Schulz, Design and Evaluation of a Low-Cost Force Feedback System for
- Myoelectric Prosthetic Hands:, *JPO J. Prosthet. Orthot.* **18**, 57–61 (2006).
- 518 25. H. J. B. Witteveen, E. A. Droog, J. S. Rietman, P. H. Veltink, Vibro- and Electrotactile User Feedback on Hand
- Opening for Myoelectric Forearm Prostheses, *IEEE Trans. Biomed. Eng.* **59**, 2219–2226 (2012).

- 520 26. E. Mastinu, P. Doguet, Y. Botquin, B. Håkansson, M. Ortiz-Catalan, Embedded System for Prosthetic Control
- Using Implanted Neuromuscular Interfaces Accessed Via an Osseointegrated Implant, IEEE Trans. Biomed. Circuits
- 522 Syst. 11, 867–877 (2017).
- 523 27. M. Ortiz-Catalan, E. Mastinu, R. Brånemark, B. Håkansson, in XVI World Congress of the International Society
- *for Prosthetics and Orthotics*, (2017).
- 525 28. H. Charkhkar, C. E. Shell, P. D. Marasco, G. J. Pinault, D. J. Tyler, R. J. Triolo, High-density peripheral nerve
- 526 cuffs restore natural sensation to individuals with lower-limb amputations, J. Neural Eng. (2018), doi:10.1088/1741-
- 527 2552/aac964.
- 528 29. D. M. Page, J. A. George, D. T. Kluger, C. Duncan, S. Wendelken, T. Davis, D. T. Hutchinson, G. A. Clark,
- 529 Motor Control and Sensory Feedback Enhance Prosthesis Embodiment and Reduce Phantom Pain After Long-Term
- Hand Amputation, Front. Hum. Neurosci. 12 (2018), doi:10.3389/fnhum.2018.00352.
- 30. G. Valle, A. Mazzoni, F. Iberite, E. D'Anna, I. Strauss, G. Granata, M. Controzzi, F. Clemente, G. Rognini, C.
- 532 Cipriani, T. Stieglitz, F. M. Petrini, P. M. Rossini, S. Micera, Biomimetic Intraneural Sensory Feedback Enhances
- 533 Sensation Naturalness, Tactile Sensitivity, and Manual Dexterity in a Bidirectional Prosthesis, Neuron 100, 37-45.e7
- 534 (2018).
- 31. J. A. George, M. R. Brinton, C. C. Duncan, D. T. Hutchinson, G. A. Clark, in 2018 40th Annual International
- Conference of the IEEE Engineering in Medicine and Biology Society (EMBC), (2018), pp. 3782–3787.
- 537 32. J. S. Hebert, J. Lewicke, Case report of modified box and blocks test with motion capture to measure prosthetic
- 538 function, J. Rehabil. Res. Dev. 49, 1163- (2012).
- 33. D. T. Beckler, Z. C. Thumser, P. D. Marasco, in MEC17 A Sense of What's To Come, (Fredericton, New
- 540 Brunswick, Canada, 2017), p. 106.
- 34. A.-S. Augurelle, A. M. Smith, T. Lejeune, J.-L. Thonnard, Importance of Cutaneous Feedback in Maintaining a
- Secure Grip During Manipulation of Hand-Held Objects, J. Neurophysiol. **89**, 665–671 (2003).
- 35. E. D. Engeberg, S. Meek, Improved Grasp Force Sensitivity for Prosthetic Hands Through Force-Derivative
- 544 Feedback, *IEEE Trans. Biomed. Eng.* **55**, 817–821 (2008).
- 36. F. Clemente, M. D'Alonzo, M. Controzzi, B. B. Edin, C. Cipriani, Non-Invasive, Temporally Discrete Feedback
- of Object Contact and Release Improves Grasp Control of Closed-Loop Myoelectric Transradial Prostheses, *IEEE*
- 547 Trans. Neural Syst. Rehabil. Eng. 24, 1314–1322 (2016).
- 548 37. D. J. O. Atkins, D. C. Y. M. Heard, W. H. Donovan, Epidemiologic Overview of Individuals with Upper-Limb
- Loss and Their Reported Research Priorities, *J. Prosthet.* **8**, 2–11 (1996).
- 38. Z. C. Thumser, A. B. Slifkin, D. T. Beckler, P. D. Marasco, Fitts' Law in the Control of Isometric Grip Force
- 551 With Naturalistic Targets, Front. Psychol. 9 (2018), doi:10.3389/fpsyg.2018.00560.
- 39. B. P. Delhaye, K. H. Long, S. J. Bensmaia, Neural Basis of Touch and Proprioception in Primate Cortex, *Compr.*
- 553 *Physiol.* **8**, 1575–1602 (2018).
- 40. R. S. Johansson, I. Birznieks, First spikes in ensembles of human tactile afferents code complex spatial fingertip
- 555 events, *Nat. Neurosci.* **7**, 170–177 (2004).
- 41. S. J. Lederman, R. L. Klatzky, Extracting Object Properties Through Haptic Exploration, Acta Psychol. (Amst.)
- **84**, 29–40 (1993).

- 42. T. Callier, A. K. Suresh, S. J. Bensmaia, Neural Coding of Contact Events in Somatosensory Cortex, Cereb.
- 559 *Cortex*, doi:10.1093/cercor/bhy337.
- 43. S. E. Hardy, in *Current Diagnosis & Treatment: Geriatrics*, B. A. Williams, A. Chang, C. Ahalt, H. Chen, R.
- 561 Conant, C. S. Landefeld, C. Ritchie, M. Yukawa, Eds. (McGraw-Hill Education, New York, NY, 2014).
- 562 44. S. S. Roley, J. V. DeLany, C. J. Barrows, S. Brownrigg, D. Honaker, D. I. Sava, V. Talley, K. Voelkerding, D.
- A. Amini, E. Smith, P. Toto, S. King, D. Lieberman, M. C. Baum, E. S. Cohen, P. A. M. Cleveland, M. J.
- 564 Youngstrom, American Occupational Therapy Association Commission on Practice, Occupational therapy practice
- framework: domain & practice, 2nd edition, Am. J. Occup. Ther. Off. Publ. Am. Occup. Ther. Assoc. 62, 625–683
- 566 (2008).
- 567 45. S. Raspopovic, M. Capogrosso, F. M. Petrini, M. Bonizzato, J. Rigosa, G. D. Pino, J. Carpaneto, M. Controzzi,
- T. Boretius, E. Fernandez, G. Granata, C. M. Oddo, L. Citi, A. L. Ciancio, C. Cipriani, M. C. Carrozza, W. Jensen,
- 569 E. Guglielmelli, T. Stieglitz, P. M. Rossini, S. Micera, Restoring Natural Sensory Feedback in Real-Time
- Bidirectional Hand Prostheses, *Sci. Transl. Med.* **6**, 222ra19-222ra19 (2014).
- 46. M. Ortiz-Catalan, B. Håkansson, R. Brånemark, An osseointegrated human-machine gateway for long-term
- sensory feedback and motor control of artificial limbs, Sci. Transl. Med. 6, 257re6-257re6 (2014).
- 573 47. S. Lewis, M. F. Russold, H. Dietl, E. Kaniusas, in 2012 IEEE International Symposium on Medical
- 574 *Measurements and Applications Proceedings*, (2012), pp. 1–4.
- 48. E. L. Graczyk, L. Resnik, M. A. Schiefer, M. S. Schmitt, D. J. Tyler, Home Use of a Neural-connected Sensory
- Prosthesis Provides the Functional and Psychosocial Experience of Having a Hand Again, Sci. Rep. 8, 9866 (2018).
- 577 49. B. Rosén, H. H. Ehrsson, C. Antfolk, C. Cipriani, F. Sebelius, G. Lundborg, Referral of sensation to an advanced
- 578 humanoid robotic hand prosthesis, Scand. J. Plast. Reconstr. Surg. Hand Surg. 43, 260–266 (2009).
- 579 50. C. Dietrich, K. Walter-Walsh, S. Preissler, G. O. Hofmann, O. W. Witte, W. H. R. Miltner, T. Weiss, Sensory
- feedback prosthesis reduces phantom limb pain: proof of a principle, *Neurosci. Lett.* **507**, 97–100 (2012).
- 581 51. M. R. Brinton, E. Barcikowski, M. Paskett, T. Davis, J. Nieveen, D. T. Kluger, J. A. George, D. J. Warren, G. A.
- 582 Clark, Development of a Take-Home System for Control of Advanced Prosthetics, Soc. Neurosci. (2018).
- 583 52. T. S. Davis, H. A. C. Wark, D. T. Hutchinson, D. J. Warren, K. O'Neill, T. Scheinblum, G. A. Clark, R. A.
- Normann, B. Greger, Restoring motor control and sensory feedback in people with upper extremity amputations
- using arrays of 96 microelectrodes implanted in the median and ulnar nerves, *J. Neural Eng.* **13**, 036001 (2016).
- 53. G. A. Clark, S. Wendelken, D. M. Page, T. Davis, H. A. Wark, R. A. Normann, D. J. Warren, D. T. Hutchinson,
- 587 in Engineering in Medicine and Biology Society (EMBC), 2014 36th Annual International Conference of the IEEE,
- 588 (IEEE, 2014), pp. 1977–1980.
- 589 54. J. G. Nieveen, Y. Zhang, S. Wendelken, T. S. Davis, D. T. Kluger, J. A. George, D. J. Warren, D. T. Hutchinson,
- 590 C. Duncan, G. A. Clark, Polynomial kalman filter for myoelectric prosthetics using efficient kernel ridge regression
- 591 (2017).
- 59. J. A. George, T. S. Davis, M. R. Brinton, G. Clark, Intuitive Neuromyoelectric Control of a Dexterous Bionic
- 593 Arm Using a Modified Kalman Filter, *J. Neurosci. Methods* (In Review).
- 56. H. P. Saal, B. P. Delhaye, B. C. Rayhaun, S. J. Bensmaia, Simulating tactile signals from the whole hand with
- 595 millisecond precision, *Proc. Natl. Acad. Sci.* **114**, E5693–E5702 (2017).
- 596 57. J. M. Goodman, G. A. Tabot, A. S. Lee, A. K. Suresh, A. T. Rajan, N. G. Hatsopoulos, S. J. Bensmaia, Postural
- Representations of the Hand in Primate Sensorimotor Cortex, bioRxiv, 566539 (2019).

- 58. E. L. Graczyk, B. P. Delhaye, M. A. Schiefer, S. J. Bensmaia, D. J. Tyler, Sensory adaptation to electrical 598
- 599 stimulation of the somatosensory nerves, J. Neural Eng. 15, 046002 (2018).
- 600 59. L. Resnik, S. L. Klinger, K. Etter, The DEKA Arm: Its features, functionality, and evolution during the Veterans
- 601 Affairs Study to optimize the DEKA Arm, *Prosthet. Orthot. Int.* **38**, 492–504 (2014).
- 60. D. R. Merrill, M. Bikson, J. G. R. Jefferys, Electrical stimulation of excitable tissue: design of efficacious and 602
- 603 safe protocols, J. Neurosci. Methods 141, 171–198 (2005).
- 61. B. Baker, R. Caldwell, D. Crosland, R. Sharma, D. Kluger, J. A. George, A. Harding, L. Reith, Improved Long-604
- 605 term Performance of Utah Slanted Arrays in Clinical Studies (2018).
- 62. D. J. Warren, S. Kellis, J. G. Nieveen, S. M. Wendelken, H. Dantas, T. S. Davis, D. T. Hutchinson, R. A. 606
- 607 Normann, G. A. Clark, V. J. Mathews, Recording and decoding for neural prostheses, *Proc. IEEE* 104, 374–391
- 608 (2016).

- 609 63. W. Wu, M. J. Black, D. Mumford, Y. Gao, E. Bienenstock, J. P. Donoghue, Modeling and decoding motor
- cortical activity using a switching Kalman filter, IEEE Trans. Biomed. Eng. 51, 933-942 (2004). 610
- 64. S. Wendelken, D. M. Page, T. Davis, H. A. C. Wark, D. T. Kluger, C. Duncan, D. J. Warren, D. T. Hutchinson, 611
- 612 G. A. Clark, Restoration of motor control and proprioceptive and cutaneous sensation in humans with prior upper-
- limb amputation via multiple Utah Slanted Electrode Arrays (USEAs) implanted in residual peripheral arm nerves, 613
- 614 J. NeuroEngineering Rehabil. 14, 121 (2017).
- 615 65. R. L. Rennaker, J. Miller, H. Tang, D. A. Wilson, Minocycline increases quality and longevity of chronic neural
- 616 recordings, J. Neural Eng. 4, L1–L5 (2007).
- 617 66. P. J. Rousche, R. A. Normann, A method for pneumatically inserting an array of penetrating electrodes into
- 618 cortical tissue, Ann. Biomed. Eng. 20, 413–422 (1992).
- 67. L. Spataro, J. Dilgen, S. Retterer, A. J. Spence, M. Isaacson, J. N. Turner, W. Shain, Dexamethasone treatment 619
- 620 reduces astroglia responses to inserted neuroprosthetic devices in rat neocortex, Exp. Neurol. 194, 289–300 (2005).
- 621 68. Y. Zhong, R. V. Bellamkonda, Dexamethasone Coated Neural Probes Elicit Attenuated Inflammatory Response
- 622 and Neuronal Loss Compared to Uncoated Neural Probes, Brain Res. 1148, 15-27 (2007).
- 69. Z. C. Thumser, A. B. Slifkin, D. T. Beckler, P. D. Marasco, Fitts' Law in the Control of Isometric Grip Force 623
- 624 With Naturalistic Targets, Front. Psychol. 9 (2018), doi:10.3389/fpsyg.2018.00560.
- 625 Acknowledgments: We thank the participant in this study who freely donated 14-months of his life for
- 626 the advancement of knowledge and for a better future for amputees. Funding: This work was
- sponsored by the Hand Proprioception and Touch Interfaces (HAPTIX) program administered by 627
- 628 the Biological Technologies Office (BTO) of the Defense Advanced Research Projects Agency
- (DARPA) under the auspices of Dr. Doug Weber, through the Space and Naval Warfare Systems 629 Center, Contract No. N66001-15-C-4017. Additional sponsorship was provided by the National
- Science Foundation (NSF) through grant No. NSF ECCS-1533649. and NSF GRFP Award No. 631
- 1747505. Author contributions: J.A. George developed and implemented sensory encoding 632
- algorithms, designed experiments, collected data and drafted the manuscript. D.T. Kluger 633
- developed software for prosthetic hand, designed experiments, collected data and assisted with 634
- drafting of the manuscript. T.S. Davis developed software for closed-loop prosthesis control. E.V. 635
- Okorokova and Q. He developed sensory encoding algorithm based on afferent recordings. C.C. 636
- Duncan provided clinical support and expertise throughout. D.T. Hutchinson implanted and 637
- 638 explanted the USEAs and iEMGs, provided clinical oversight throughout the study, and oversaw

development of experiments and protocols. Z.C. Thumser, D.T. Deckler and P.D. Marasco provided equipment and guidance for GRIP and PEP tests. S.J. Bensmaia oversaw development of sensory encoding algorithms, assisted in experimental design and aided with drafting of the manuscript. G.A. Clark oversaw and led development of all methods, experiments, and protocols, and assisted with experiments and drafting of the manuscript. All authors contributed to the revision of the manuscript. **Competing interests**: Authors DK, TD, SW, CD, and GC are inventors of the prosthetic control algorithm used in this study (International Application No. PCT/US2017/044947). DK, SW, DH, and GC are inventors of the protective carrier devices used during the implant procedure (International Application No. PCT/US2017/044427). GC holds patents on the implants' signal referencing and anti-noise architecture (US Patent Nos. 8639312 and 8359083). TD is a consultant for Ripple, LLC. **Data and materials availability**: Data requests should be sent to Gregory Clark (greg.clark@utah.edu). Requestors may need to be approved by the human-subjects research committees (e.g., local IRB and DoN-HRPP) in order to comply with HIPAA requirements.

Figure and Table Captions:

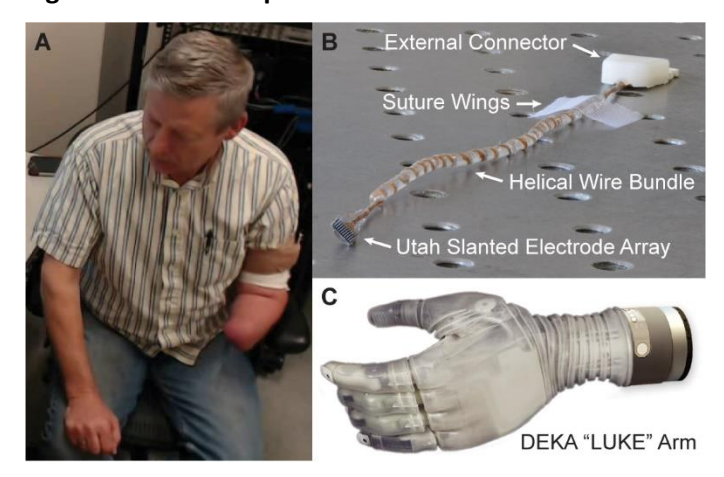


Fig. 1. Subject and sensitized bionic hand. A transradial amputee **(A)** had two total Utah Slanted Electrode Arrays (USEAs) **(B)** implanted, one each, into the residual median and ulnar nerves of the arm. Activation of contact sensors on the DEKA "LUKE" Arm **(C)** triggered stimulation of individual USEA electrodes or groups of USEA electrodes so that the amputee felt a sensation on his phantom hand at the corresponding location. For example, when contact was made with the index fingertip sensor, current was delivered through USEA electrodes with projection fields on the phantom index fingertip. Thus, when the prosthetic index fingertip made contact with an object, the participant experienced a sensation on the index fingertip.

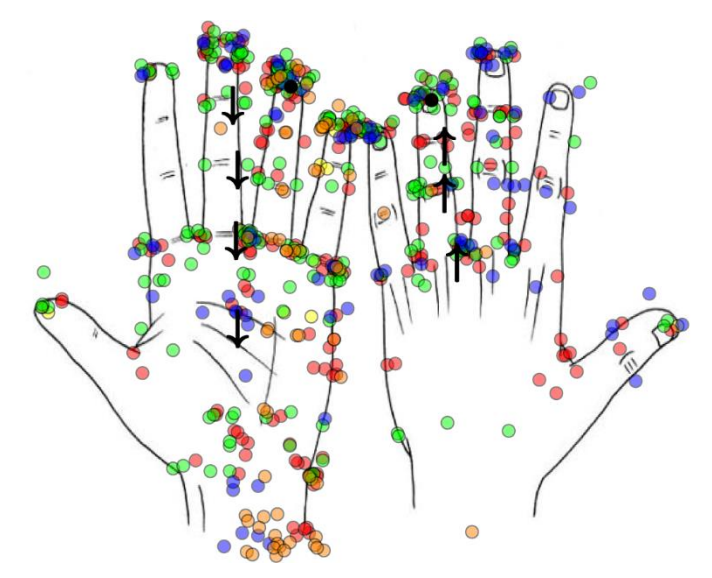


Fig. 2. Centroids of the projected fields for cutaneous percepts (circles & squares) and location of proprioceptive percepts (black arrows) evoked by stimulation through individual USEA electrodes in the residual median (circles) or ulnar (squares) nerves. A total of 119 sensory percepts were evoked (72% from median nerve) two weeks after the implantation surgery. The quality of the evoked percepts varied across electrodes: 37% vibration (red), 29% pressure (green), 16% pain (blue), 12% tightening (orange), 3% movement (arrows), 3% tapping (yellow), 1% buzzing (black). A map of the complete projected fields can be found in Fig. S3.

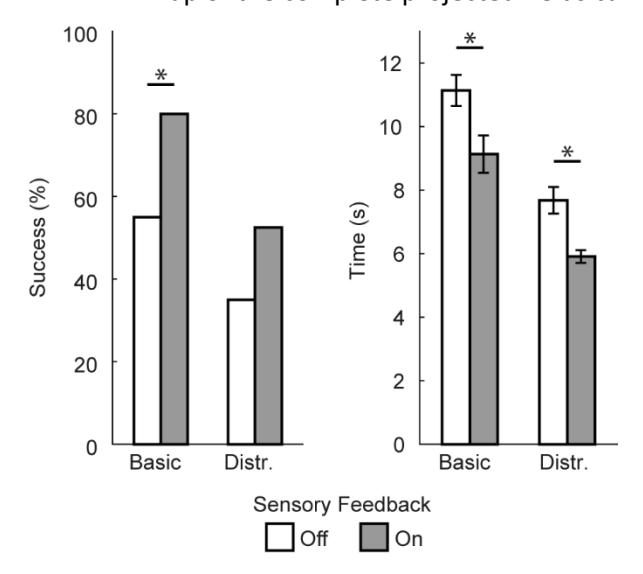


Fig. 3. Sensory feedback improves object manipulation. The subject's task was to move a "fragile" object, which breaks if the grip force is too strong. With sensory feedback, the participant moved the object more often without breaking it and did so more rapidly (Basic). With divided attention (Distr.), the feedback-induced boost in performance was maintained, but only the effect on duration remained statistically significant. * p < 0.05, N = 80 for both Basic and Distr. cases. Data show mean \pm S.E.M.

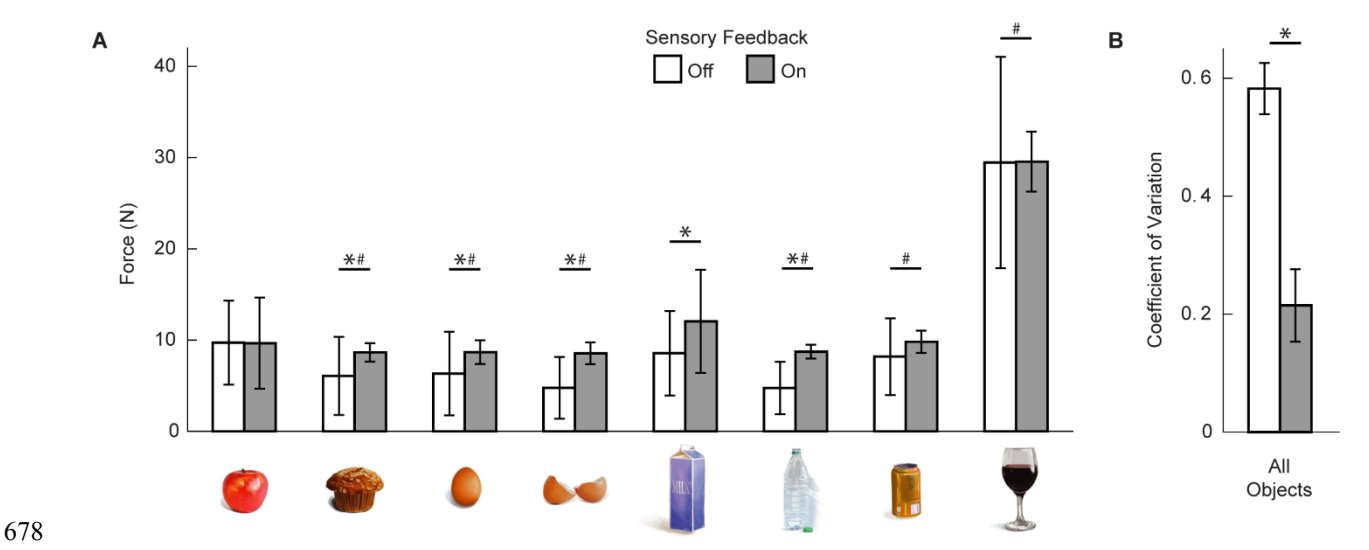


Fig. 4. Sensory feedback improves grip precision. **(A)** Forces (mean \pm standard deviation) generated by the participant when grasping of a load cell while viewing one of eight different virtual objects. Sensory feedback improved grip precision, as evidenced by less variable grip force on 6 of 8 objects. Without sensory feedback, the participant erred on the side of caution and underestimated desired grip force for fragile objects (bread, eggs, open water bottle). **(B)** Coefficient of variation (mean \pm S.E.M.) of grip force across all 8 objects. Sensory feedback significantly reduced the coefficient of variation (i.e., the ratio of grip precision to grip force). * different means (p < 0.05); # different standard deviations (p < 0.05); N = 40 for each object.

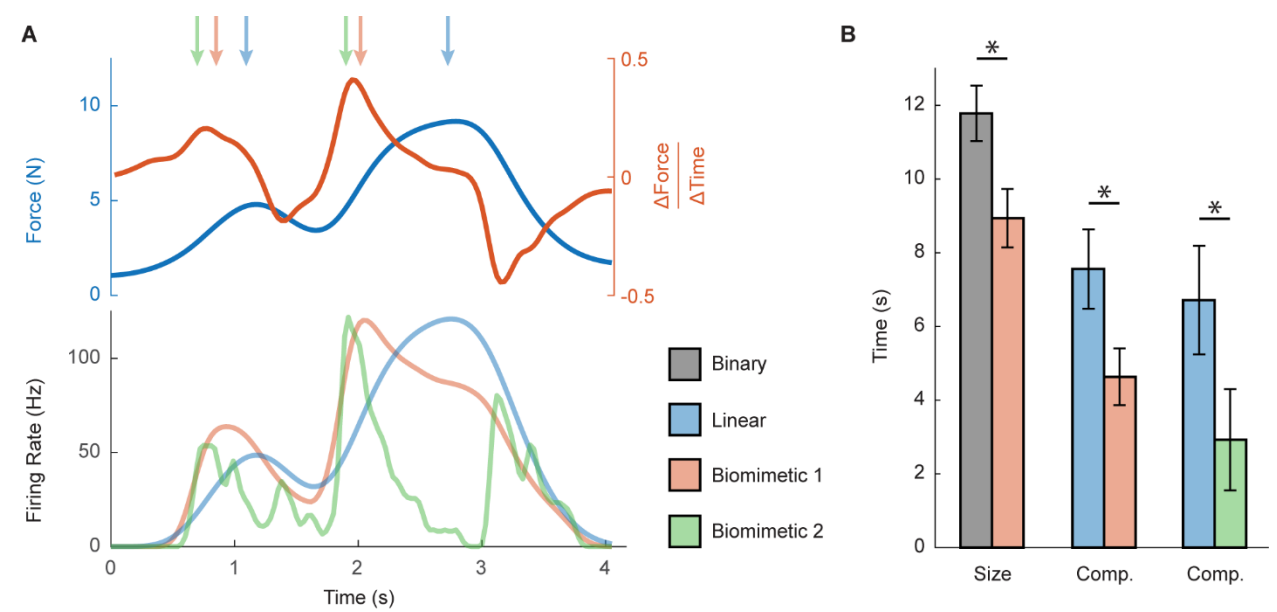


Fig. 5. Biomimetic sensory feedback improves performance on object discrimination tasks. (A) Example force (top, blue) and change in force (top, red) when the participant actively manipulated a soft foam block. Note the repetitive waxes and wanes in force (e.g., at ~ 2s), associated with the participant's active exploration of the object. Traditional linear encoding tracks force only (bottom, light blue), whereas the first order biomimetic encoding incorporates the first derivative of force (bottom, light red) and second order biomimetic mimics the aggregate responses of tactile nerve fibers (bottom, light green). Linear algorithms were scaled (doubled) such that peak

stimulation amplitude and frequency were matched to the biomimetic algorithms; arrows highlight the time when peak stimulation occurs for the different algorithms. **(B)** Biomimetic sensory feedback improved response time relative to its non-biomimetic counterpart in size and compliance (comp.) discrimination tasks. Performance across experiments varied due to changes in stimulation parameters, but biomimetic stimulation consistently outperformed non-biomimetic stimulation. * p < 0.05, N = 32 for binary vs biomimetic 1, N = 48 for linear vs biomimetic 1, and N = 32 for binary vs biomimetic 2. Data show mean \pm S.E.M.



Fig. 6. Sensory feedback supports activities of daily living (ADLs). The participant performed several one-and two-handed ADLs while using the sensorized prosthesis, including: moving an egg **(A)**, picking grapes **(B)**, texting on his phone **(C)**, and shaking hands with his wife **(D)**.

Table 1. Stimulation parameters used for each task.

Task	Sensory Encoding Algorithm(s)	USEA Electrodes	Amplitude (μΑ)	Frequency (Hz)	Duration (μs)
Fragile object (first set)	Traditional Linear	2, 5, 6, 9, 10, 12, 15, 16, 20, 25	80 – 100	10 – 100	200
Fragile object (second set)	Traditional Linear	2, 5, 6, 9, 10, 12, 15, 16, 20, 23, 25	70 – 100	10 – 100	200
GRIP	1° Biomimetic	5, 6, 9, 10, 12, 15, 16, 20, 23	80 – 95	10 – 200	320

		ı	ı	1	
Size Discrimination	1° Biomimetic	2, 5, 6, 9, 10, 12, 15, 16, 20, 23	80 – 95	10 – 200	200
Size Discrimination	Binary	5, 6, 9, 10, 12, 15, 16, 20, 25, 26	100	100	320
Compliance Discrimination (first set)	1° Biomimetic vs Traditional Linear	2, 5, 6, 9, 10, 12, 15, 16, 20, 23	90 – 100	10 – 200	200
Compliance Discrimination (second set)	1° Biomimetic vs Traditional Linear	2, 5, 6, 9, 10, 12, 15, 16, 20, 23	80 – 95	10 – 200	320
Compliance Discrimination (first set)	1° Biomimetic vs Scaled Traditional Linear	2, 5, 6, 9, 10, 12, 15, 16, 20, 23	80 – 95	10 – 200	320
Compliance Discrimination (second set)	1° Biomimetic vs Scaled Traditional Linear	5, 6, 9, 10, 12, 15, 16, 20, 23, 25, 26	80 – 100	10 – 200	320
Compliance Discrimination	2° Biomimetic vs Scaled Traditional Linear	5, 6, 9, 10, 12, 15, 16, 20, 23, 25, 26	70	10 – 400	320
Activities of Daily Living (first set)	Traditional Linear	23, 26, 33, 41, 42, 47, 63	70 – 100	10 – 100	200
Activities of Daily Living (second set)	Traditional Linear	23, 26, 27, 33, 34	60 – 100	100	200
Activities of Daily Living (third set)	Traditional Linear	9, 10, 20	80 – 100	10 – 100	200

Table 2. Sensory encoding algorithms.

Sensory Encoding Algorithm(s)	Analytic Formulation
Binary	$F_t = F_{min}$

	$A_t = A_{min}$
Traditional Linear	$F_t = C_t(F_{max} - F_{min}) + F_{min}$ $A_t = C_t(A_{max} - A_{min}) + A_{min}$
Scaled Traditional Linear	$F_t = 2C_t(F_{max} - F_{min}) + F_{min}$ $A_t = 2C_t(A_{max} - A_{min}) + A_{min}$
Biomimetic 1	$F_{t} = \begin{cases} C_{t}(F_{max} - F_{min}) + F_{min}, V_{t} < 0 \\ (5V_{t} + C_{t}) * (F_{max} - F_{min}) + F_{min}, V_{t} \ge 0 \end{cases}$ $A_{t} = \begin{cases} C_{t}(A_{max} - A_{min}) + A_{min}, V_{t} < 0 \\ (5V_{t} + C_{t}) * (A_{max} - A_{min}) + A_{min}, V_{t} \ge 0 \end{cases}$
Biomimetic 2	$F_t = 186C_t - 185C_{t-1} + 1559V_t - 360V_{t-1} - 109V_{t-2} + 364A_t + 170A_{t-1} - 3$ $A_t = A_{min}$

 F_t : Frequency at time t. A_t : Amplitude at time t. C_t : Normalized contact value at time t. V_t : Velocity at time t. A_t : Acceleration at time t. M_t : Minimum value. M_t : Maximum value.

Note: For all algorithms, sensory feedback is off and no stimulation occurs when $\mathcal{C}_t=0.$

708 **Table 3.** Motor Control Specifications

DOF	Range	Precision	Angle at rest
Thumb adduction/abduction	0–75°	0.08 °/bit	22.5°
Thumb reposition/opposition	50–100°	0.10 °/bit	80°
Index extend/flex	0–90°	0.09 °/bit	27°
MRP extend/flex	0–90°	0.09 °/bit	27°
Wrist supinate/pronate	-120–175°	0.29 °/bit	0°
Wrist extend/flex	-55–55°	0.11 °/bit	0°

Table 4. Sensor Specifications

Sensor	Range	Precision
Thumb adduction/abduction	0–75°	2.08 x 10 ⁻⁴ °/bit
Thumb reposition/opposition	0–100°	1.56 x 10 ⁻⁴ °/bit
Index extend/flex	0–90°	1.74 x 10 ⁻⁴ °/bit
MRP extend/flex	0–90°	1.74 x 10 ⁻⁴ °/bit
Wrist supinate/pronate	-120–175°	5.30 x 10 ⁻⁵ °/bit

Wrist extend/flex	-55–55°	1.42 x 10 ⁻⁴ °/bit
All contact sensors	0–25.6 N	0.1 N/bit

Supplemental Materials and Methods:

Stability of electrically evoked percepts

Every 4–8 weeks, we mapped the location, quality, and intensity of the electrically elicited percept. Specifically, we stimulated through each electrode of the USEAs in isolation at increasing amplitudes. We delivered stimulation in a pulsed fashion: a 500-ms, 100-Hz stimulation train was delivered every second. We identified perceptual thresholds by increasing stimulation current at 1–10 μ A steps until a sensation was reported (Fig. S8). Electrodes that did not evoke a percept below 100 μ A were not included in the stability analyses. To quantify stability, we compared the projection fields for each electrode at adjacent timepoints. We define percent stable as the number of electrodes with consistent projection fields between the current timepoint and the previous timepoint out of the total number of electrodes that evoked sensations at both timepoints. For quantifying electrode impedance, we considered all working electrodes (i.e., electrodes with visibly intact wires and impedances below 500 k Ω), even if they did not evoke a percept on that particularly day. Because the data were not normally distributed, we performed statistical analyses using separate one-way ANOVAs on ranks (Kruskal-Wallis).

Due to wire breakage associated with the percutaneous implants, the number of working electrodes and individual electrodes that evoked a percept diminished across the 14-month duration of the study (Fig. S8). Stability analyses are limited to the first 298 days. After 354 days post implantation, individual electrodes were unable to evoke sensations on their own, and instead simultaneous stimulation across multiple working electrodes was used to evoke sensations. In the present experiments, the USEA provided a unique opportunity to explore the functional benefits of biomimetic sensory feedback. Improvements to the longevity of the USEA are ongoing (61) and 17-month neural recordings have since been demonstrated in a more recent amputee participant (55).

Decoding intended movements with a modified Kalman filter

The MKF control algorithm used in this study is described in detail in (55) and is only summarized here.

Continuous electromyographic signals (32 channels) were band-pass filtered with cutoff frequencies of 15 Hz (sixth-order high-pass Butterworth filter) and 375 Hz (second-order low-pass Butterworth filter). Notch filters were also applied at 60, 120, and 180 Hz. Differential EMG signals were calculated for all possible pairs of channels, resulting in 496 (32 choose 2) differential pair recordings. The mean absolute value (MAV) was then calculated for the 32 single-ended recordings and the 496 differential recordings at 30 Hz. The MAV was smoothed using an overlapping 300-ms window. The resulting electromyographic feature set consisted of the 300-ms smoothed MAV on 528 channels (32 single-ended channels and 496 differential pairs), calculated at 30 Hz.

We used a standard Kalman filter (62, 63) to estimate motor intent from continuous electromyographic signals, similar to what we previously reported in ref. (64). The baseline MAV for each channel was subtracted from the features prior to training and testing of the Kalman filter. A subset of 48 channels was then selected using a stepwise Gram-Schmidt channel-selection algorithm (54). We bound the output of the Kalman filter between -1 and 1 to match the limits of the DEKA "LUKE" Arm (64). In position control, -1 corresponded to maximum extension/adduction/supination, +1 corresponded to maximum flexion/abduction/pronation, and the hand was at rest at zero. In velocity control, -1 corresponded to

maximum velocity towards extension/adduction/supination, +1 corresponded to maximum velocity towards flexion/abduction/pronation, and the hand was at rest at zero.

Additionally, the output of the Kalman filter was modified using ad-hoc thresholds and non-uniform gains (55). These thresholds and gains were tuned by the experimenter on a DOF-by-DOF basis guided by participant feedback. The modified output was then used to directly control the position or velocity of the prosthesis at 30 Hz. Although the computational time required for the modified Kalman filter (using just electromyographic features) is only ~10 ms, a fixed 30-Hz closed-loop control rate was used to provide additional time for real-time visualization, sensory encoding, and data storage. Details regarding the accuracy of MKF at decoding motor intent are covered in greater detail in (31, 55).

Surgical Procedure

The surgical procedures to implant the USEAs are described in detail in (29) and only summarized here.

The subject was given an oral prophylactic antibiotic (100 mg minocycline, seven days, twice per day, starting the day before implant), which has been reported to improve neuronal recording quality (65). Under general anesthesia, iEMGs were implanted midway along the forearm with attempted targeting of each lead to different lower-arm extensor or flexor muscles. The epineurium was dissected from the median and ulnar nerves in the upper arm, several centimeters proximal to the medial epicondyle. USEAs were pneumatically inserted into the nerves (66) so the slanted aspect of the USEA ran along the length of the nerve (to ensure full cross-sectional coverage). If enough epineurium was available, it was sutured back together around each USEA. Collagen wraps (AxoGuard Nerve Protector, Axogen, Alachua, FL, USA) were then secured around the nerve and the ground and reference wires with vascular clips. A 0.1 mg/kg dose of dexamethasone was administered after tourniquet removal, which has been reported to reduce the foreign body response and improve neural recordings (67, 68).

The percutaneous wire sites were dressed using an antibiotic wound patch (Biopatch, Ethicon US LLC, Somerville, NJ, USA) and replaced at least once a month. The USEAs and iEMGs were surgically removed after 14 months as the result of prior mutual agreements between the volunteer participants and the experimenters regarding study duration.

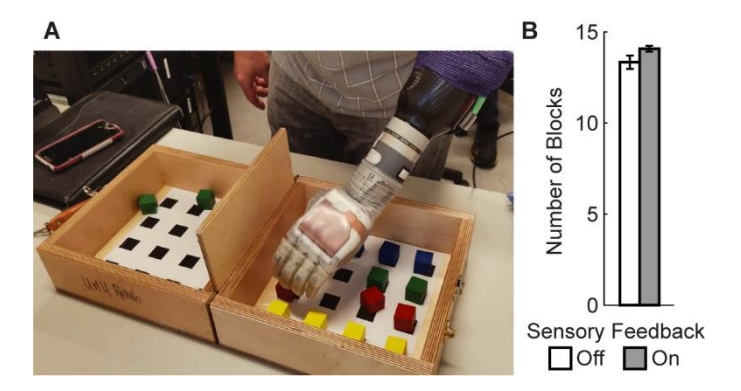


Fig. S1. "Modified Box and Blocks" test. (A) Still picture of the participant performing the task (32), a clinical test of hand dexterity. (B) Sensory feedback did not significantly improve the participants score

because visual feedback was provided and no penalty was incurred for handling the blocks forcefully. N = 10 trails. Data show mean \pm S.E.M.

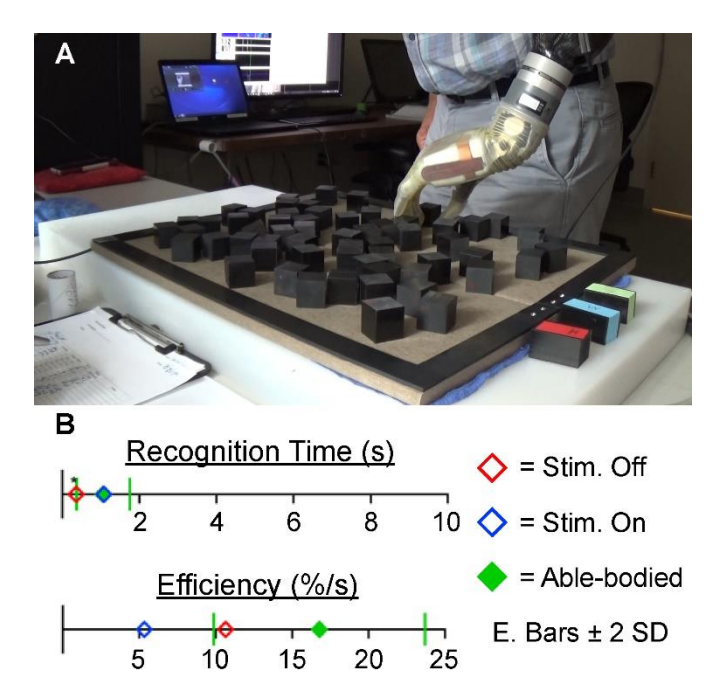


Fig. S2. Prosthesis Efficiency and Profitability task (33). **(A)** Participant foraged for blocks of a certain compliance as fast as possible. **(B)** The participant's low recognition times and high efficiency score serve as demonstrations of strong motor capabilities. However, artificial tactile feedback did not improve performance, as the participant relied primarily on this motor output and visual feedback to complete the foraging task, and chose to focus on speed rather than accuracy.

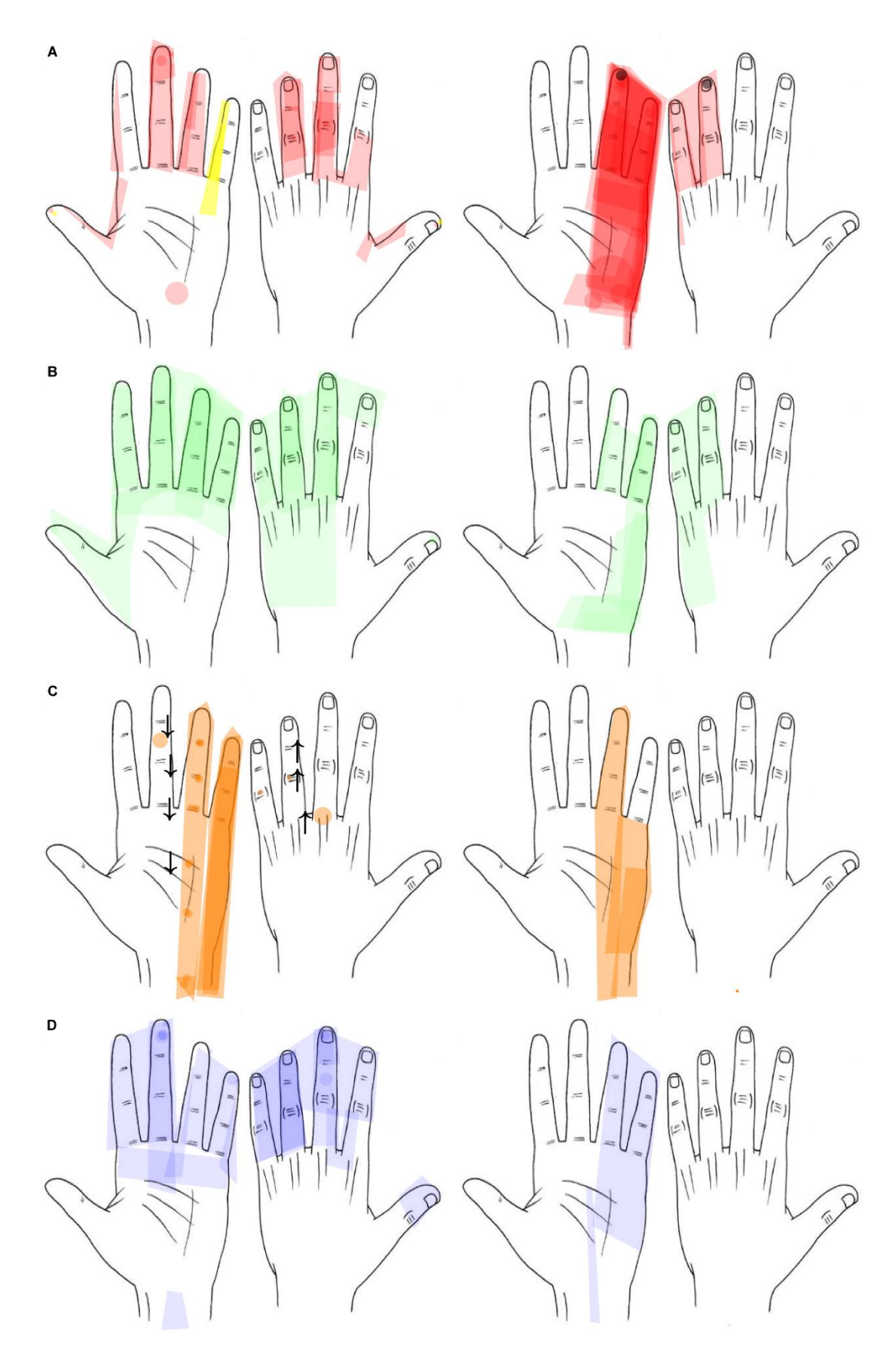


Fig. S3. Projected fields of electrically-evoked sensations. Sensory percepts were evoked by stimulation of single USEA electrodes in the residual median (left side) or ulnar (right side) nerves. A total of 119 sensory percepts were evoked (72% from median nerve) two weeks after the implantation surgery. Percept modality varied across electrodes: **(A)** 37% vibration (red), 3% tapping (yellow), 1% buzzing (black); **(B)** 29% pressure (green); **(C)** 12% tightening (orange), 3% movement (black arrows); **(D)** 16% pain (blue). Projected fields, sometimes as small as pinpoint sensations on the fingers, are transparent and overlaid such that darker colors represent redundant coverage.

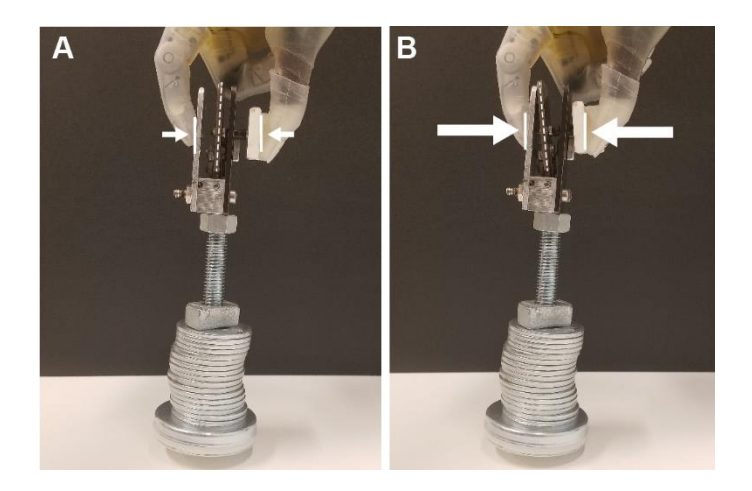


Fig. S4. Fragile-object task. **(A)** The object lifted in its "unbroken" state (applied force $< 14.79 \pm 0.34$ N, mean \pm S.E.M.). **(B)** The object lifted in its "broken" state. Breaking the object results in an audible click.

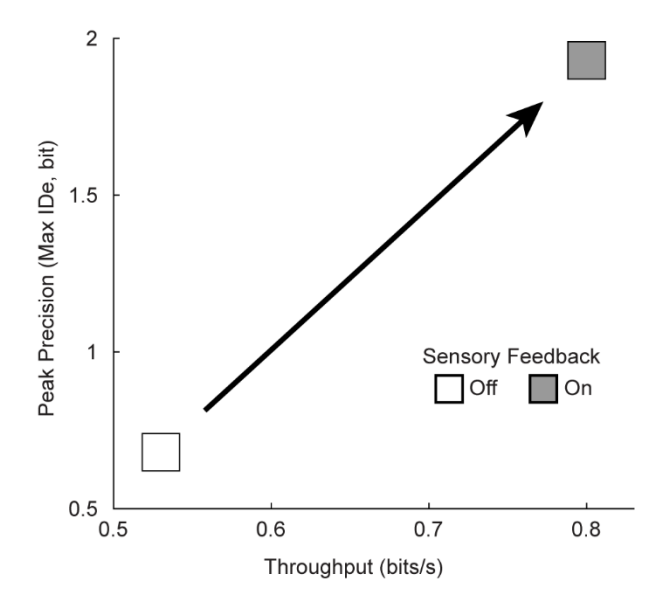


Fig. S5. Grasping Relative Index of Precision task. Sensory feedback improved the participants grip precision (y-axis) and throughput (x-axis). Additional details regarding the GRIP test can be found in *(69)*.

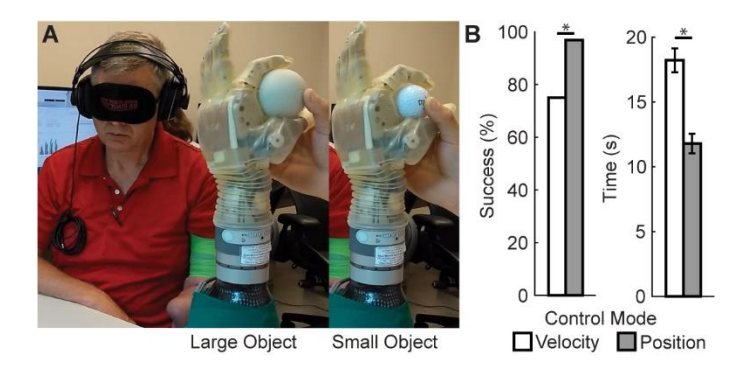


Fig. S6. Size-discrimination task. **(A)** The participant used electromyographic signals from residual arm muscles to move the prosthetic hand and manipulate a large lacrosse ball or a small golf ball. Artificial sensory feedback from USEA stimulation of residual nerves was driven by sensors on the prosthetic hand. **(B)** Postural (position) control provided better discrimination performance and speed, consistent with natural encoding scheme of the brain (57). * p < 0.05, N = 64 trials. Data show mean \pm S.E.M.

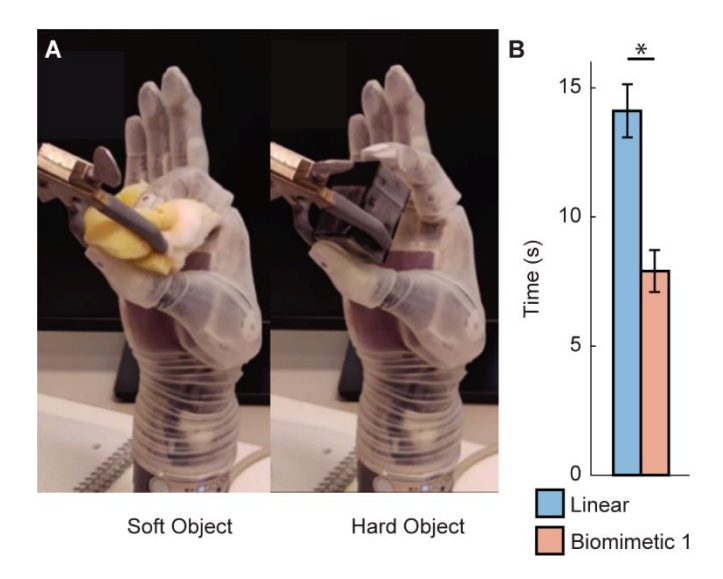


Fig. S7. Compliance-discrimination task. **(A)** The participant discriminated between a soft foam block and a hard plastic block in a closed-loop sensorimotor task. **(B)** Biomimetic sensory feedback, which resulted in a higher peak stimulation (pulse amplitude and frequency), significantly improved discrimination time. See (Fig. 5) for a comparison of biomimetic and non-biomimetic algorithms when peak stimulation is matched. * p < 0.05, N = 32 trails. Data show mean \pm S.E.M.

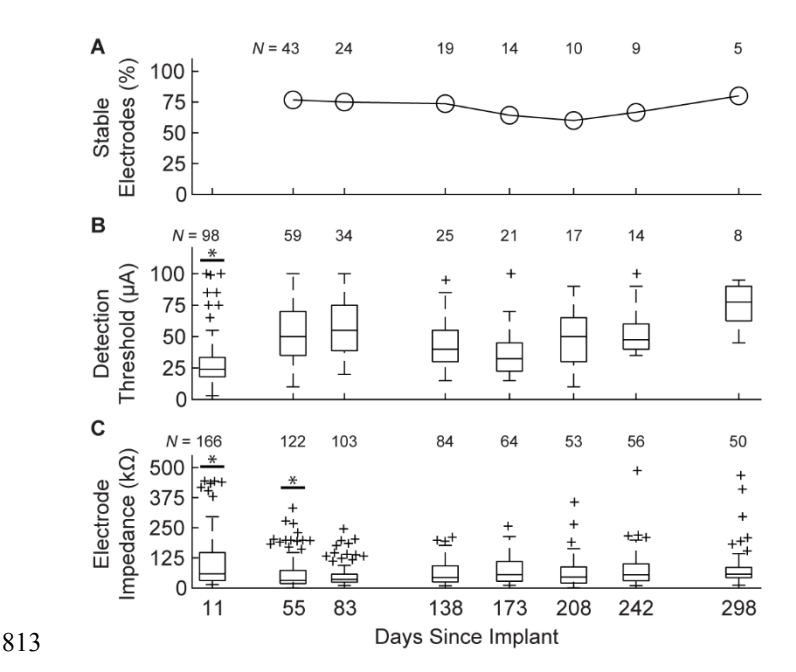


Fig. S8. Stability of USEA-evoked sensations. Artificial sensations were evoked by stimulating residual arm nerves through individual electrodes on implanted Utah Slanted Electrode Arrays. **(A)** Between 60 – 80% of artificial sensations were stable over the 298 days of testing. **(B)** Detection thresholds were stabilized after 11 days. **(C)** The impedance of working electrodes stabilized after 55 days. Box plots show median, IQR, and minimum/maximum non-outlier values. The total number of samples (*N*) is shown above each box plot. + denotes outliers outside 1.5 times the IQR. * denotes significance differences as determined by a one-way ANOVA on ranks followed by subsequent pairwise comparisons with correction. Detection threshold at day 11 was significantly different from days 55, 83, 138, 242, and 298. Impedance at day 11 was significantly different from days 55, 83, and 208. Impedance at day 55 was also significantly different from day 298. No other significant differences were found.